

Numerical study on the effect of real gas model on the flow structure and shock location of Laval nozzle

Bashar I Jasem^{1,a*} and Esam I Jassim^{2,b}

¹Department of Computer Technology, Al-Hadba University College, Mosul, Iraq.

²College of Engineering, Prince Muhammad Bin Fahd University, 31952 Al-Khobar, Kingdom of Saudi Arabia.

^aadamalzuhairi@gmail.com, ^bejassim@pmu.edu.sa

Keywords: CFD, Real Gas, Supersonic Flow, Laval Nozzle, Shock Wave

Abstract. Design of supersonic nozzle requires accurate and robust procedure since the flow becomes subtle during shifting from subsonic to supersonic. This article presents some aspects of the fluid features at supersonic region when it behaves as real gas using 3D-numerical simulation. The objectives include the variation in the shock position, the fluid properties, and the real gas model at different Nozzle-Pressure-Ratio (NPR). Results of CFD simulation showed that ideal gas model predicts higher Mach number than any real gas model. Also, the prediction is different between SRK and BWR models. The erroneous in predicating Mach number approaches 21% for SRK and 43% for BWR. For the range of NPR 2-3, shock position is found to be proportion to NPR; however, significant discrepancy in the shock location is observed when ideal gas verses real gas is assumed.

Introduction

Natural Gas is one of the prominent energy sources in industries and domestic consumption. The transportation from its sources of production to processing areas is one of the greatest challenges that transportation technology encountered [1]. Hence, research on enhancement the transportation equipment and process treatment to minimize the energy loss is still in demand. One of these devices used for purification natural gas during transportation is the convergent-divergent type nozzle, usually known as a De-Laval nozzle.

De-Laval nozzle was named after Gustaf de Laval, a Swedish inventor in 1888, [2]. The convergent divergent nozzle consists of three parts: the first part is known as the convergent or the subsonic part, where the gas velocity is accelerating, but at subsonic zone ($M < 1$). The fluid in this part is accompanied by a decrease in pressure and temperature. The second part is the throat area, where the gas velocity approaches the sound velocity ($M = 1$). The last part is the divergent part, where the velocity of the gas exceeds the sound speed and becomes supersonic ($M > 1$), [3].

Recent industrial on gas purification processes are in demand in compact design of equipment to overcome the perpetual problems of traditional means [4]. Supersonic nozzle was introduced to be an excellent alternative equipment due to its flexibility and feasibility to prevent any fouling or deposition of undesired particles, [5].

The features of shockwave region have been reported by numerous authors; however, most of these methods were developed mainly for perfect gas assumption, [4]. The assumption that the thermodynamic properties of the fluid do not significantly affect the performance of the system could lead to mislead in predicting design parameters, particularly when the supersonic fluid is made of multi-component gas mixture [6].

A good numerical model to account for real gas effects should satisfy some basic requirements, including accuracy in predicting thermodynamic properties of the fluid, capability of dealing with a wide range of state parameters, and effective and time-efficient implementation for computational fluid dynamics (CFD) analyses.

Kouremenos (1986) [7] study on normal shock reported that significant discrepancy in fluid properties was obtained when ideal gas is considered. Arina (2004) [8] numerically tested three models of real gas using CFD code. Van der Waals (VW) equation was developed in 1873 and was used by Ginzburg (1939) and later by Bai-Shi-I (1961) [9] during investigation of gas stream in nozzles. After development of Redlich-Kwong (RK) equation in 1949, a third parameter have been added to increase the accuracy of the compressibility factor. The new equation developed by Soave, Redlich, and Kwong (Soave, 1972) and Peng and Robinson (1976) is nowadays called “the cubic EOS”. To encompass wide range of pressure and temperature, Benedict-Webb-Rubin (BWR) equation and its modification (MBWR) are introduced and have proven to be quite accurate [2].

Mathematical modeling

Analysis of shock location in a Laval nozzle has been reported in numerous literatures. Jassim [10] derived a theoretical 1-D expressions that relates the Nozzle Pressure Ratio (NPR), which refers to the ratio between the local static pressure and the total pressure, to the shock location w.r.t. the nozzle throat. Here we lists the final equation (Eq.1) and one can return to ref.[10] for more details.

$$M_2 = \left[\frac{1 + [\gamma - 1/2] M_1^2}{\gamma M_1^2 - (\gamma - 1)/2} \right]^{1/2} \tag{1}$$

Numerical modeling

When selecting a numerical model to represent the state of gas flow through the nozzle, must be cover the basic requirements of the fluid including accuracy in predicting thermodynamic properties of the fluid, capability of dealing with a wide range of state parameters, and effective and time-efficient implementation for computational fluid dynamics (CFD) analyses. To analyze the shock wave that occurs, six properties of the gas flowing through the nozzle must be calculated, pressure, temperature, enthalpy, entropy, density, and velocity.

ANSYS 18 is employed to simulate the convergent-divergent nozzle, illustrated in Fig. (1), and its dimensions is listed in table (1). The 3D compressible steady state flow and energy equations are discretized to evaluate the air thermal properties while streaming along the convergent and the divergent parts.

The continuity equation in 3D form can be written as:

$$\frac{\partial}{\partial x_i} (\rho u_i) = 0 \tag{2}$$

Conservation of momentum for steady compressible flow is defined as:

$$\frac{\partial}{\partial x_i} (\rho u_i u_j) = -\frac{\partial p}{\partial x_i} + \left[\mu \left(\frac{\partial u_i}{\partial x_j} + \frac{\partial u_j}{\partial x_i} - \frac{2}{3} \delta_{ij} \frac{\partial u_l}{\partial x_l} \right) \right] + \frac{\partial}{\partial x_j} (\rho \acute{u}_i \acute{u}_j) \tag{3}$$

The 3D energy equation takes the form:

$$\frac{\partial}{\partial x_i} [u_i (\rho E + p)] = \frac{\partial}{\partial x_j} \left[\mu \left(k + \frac{c_p \mu_t}{0.85} \frac{\partial T}{\partial x_j} + u_i (-\rho \acute{u}_i \acute{u}_j) \right) \right] \tag{4}$$

The abovementioned 3 equation are solved by ANSYS-FLUENT for each grid together with the following *k-ε* equations:

$$\frac{Dk}{Dt} = \frac{\partial}{\partial x_j} \left[\left(v + \frac{v_t}{\sigma_k} \right) \frac{\partial k}{\partial x_j} \right] - \langle u'_i u'_j \rangle \frac{\partial u_i}{\partial x_j} - \varepsilon$$

$$\frac{D\varepsilon}{Dt} = \frac{\partial}{\partial x_j} \left[\left(v + \frac{v_t}{\sigma_\varepsilon} \right) \frac{\partial \varepsilon}{\partial x_j} \right] - C_{\varepsilon 1} \frac{\varepsilon}{k} \langle u'_i u'_j \rangle \frac{\partial u_i}{\partial x_j} - C_{\varepsilon 2} \frac{\varepsilon^2}{k}$$

$$v_t = C_\mu \frac{k^2}{\varepsilon}$$

System Design and fluid properties:

The Laval nozzle shown in figure (1) is constructed using DesignModeler software, a modeler embedded in ANSYS. The convergent part is 8 cm inlet diameter and 4 cm long while the divergent part is 4 cm diameter at outlet and 11 cm long. The throat diameter is 2 cm. Air is used in the simulation as working fluid and streamed axially from the convergent inlet. The properties of the working fluid is calculated based on the gas model selected, namely: Ideal gas, SRK, and BWR models.

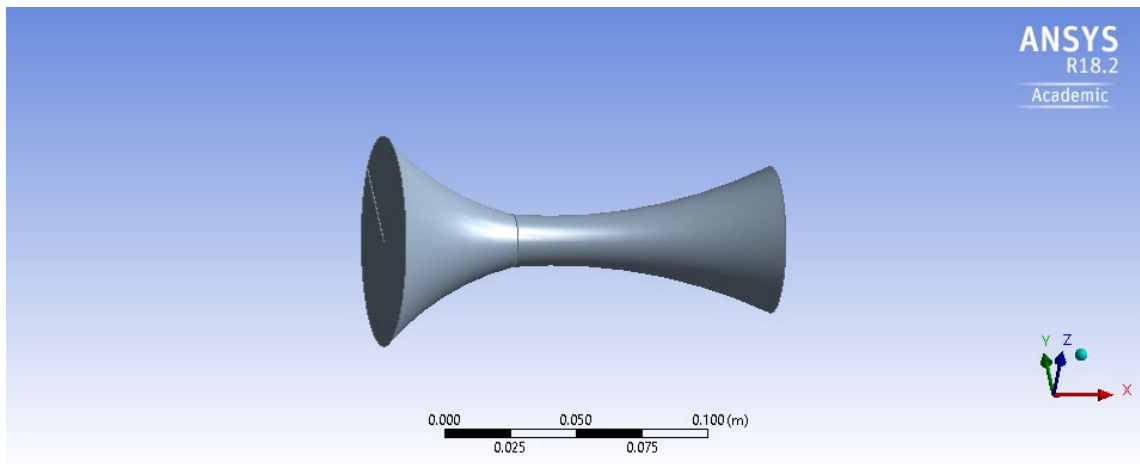


Figure 1. Geometry of the Laval Nozzle used in the simulation

Mesh architecture and dependency

Unstructured tetrahedral cell is used to construct the nozzle, considering higher grid density in the divergent part (Fig. 2). Such dense guarantees improvement of capturing the shock at the right location. The number of elements for optimal resolution was 135054, which captured the fluid structure near shock region at reasonable resolution. Mesh dependency near shock was performed and it was found that the recommended grid size should be within 0.1 mm while up to size of 1 mm was acceptable for the other regions. Since the flow is turbulent, a *k-ε* two turbulent equation was activated and solved simultaneously with the continuity, momentum, and energy equation for each element at steady state condition.

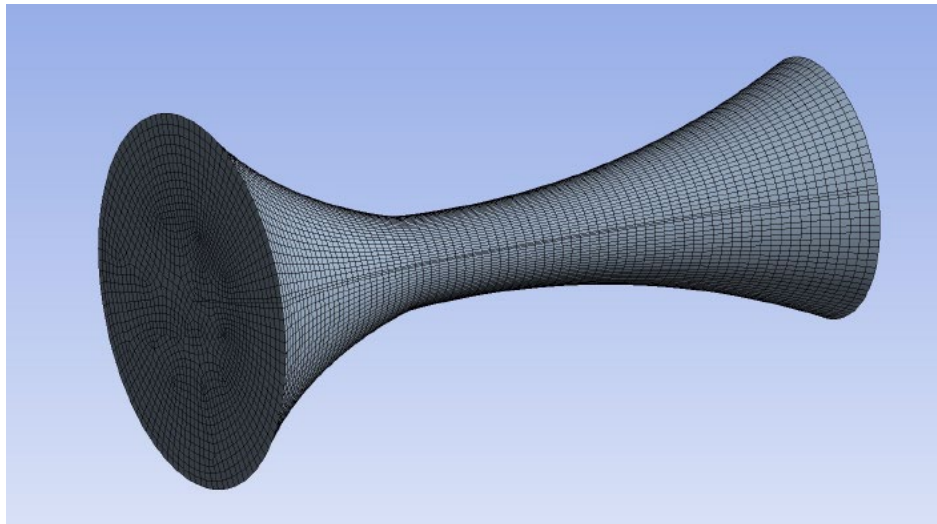


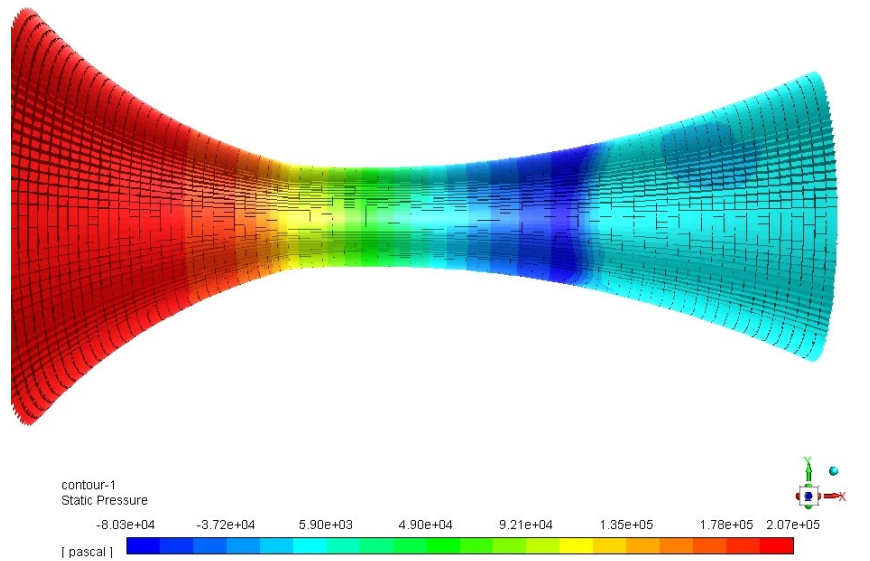
Figure 2. Unstructured mesh for better resolution

Results and discussion

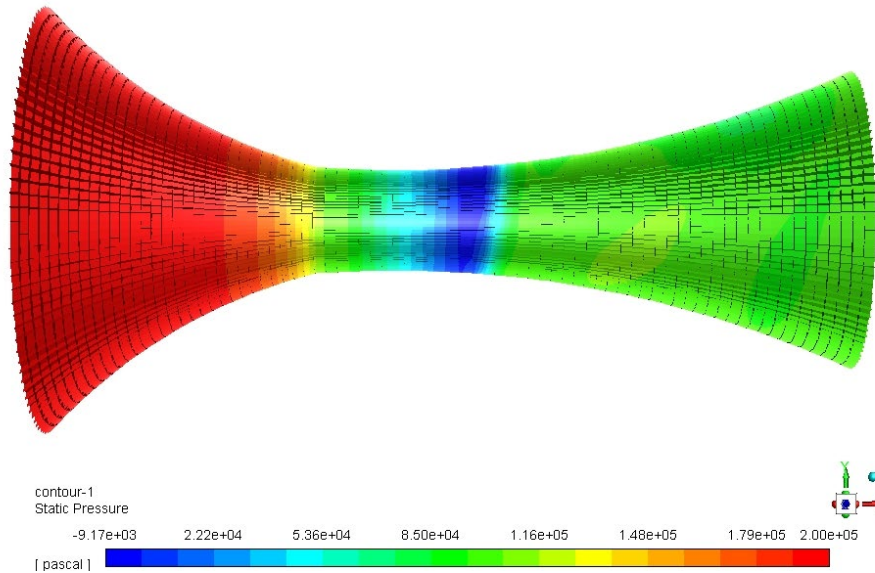
Simulation is performed for Nozzle Pressure Ratio NPR of 3/1 at three cases the ideal-gas model and two real-gas models namely SRK, and The Benedict-Webb-Rubin (BWR) equation models. The target parameters of the study are the shock location as well as the quantity of Mach number and static temperature at various NPRs. However, it is more convenient to firstly present the contours of the abovementioned parameters.

Contours of static Pressure, static temperature and Mach number

Figure 3 depicts the contour of static pressure, in gauge scale, for the ideal gas and BWR models. The minimum pressure predicted when the model of ideal gas is incorporated approaches 6% of the total pressure while not less than 30% the minimum static pressure is estimated by BWR real gas model.



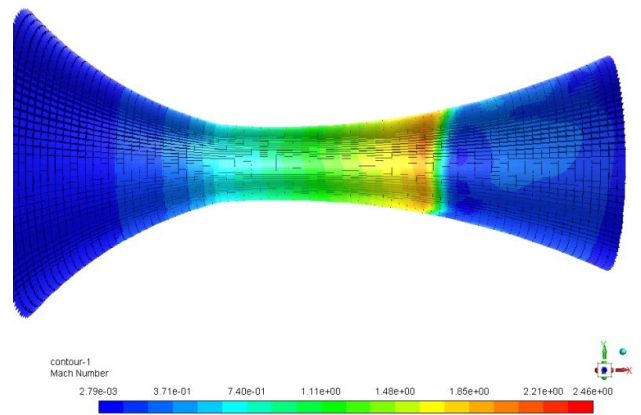
(a) Ideal gas model



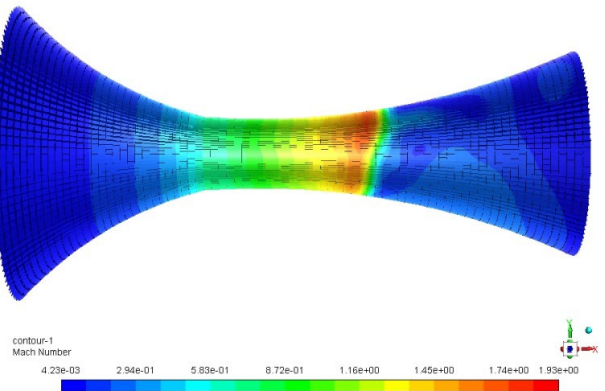
(b) BWR model

Figure 3. Contours of static pressure along the nozzle

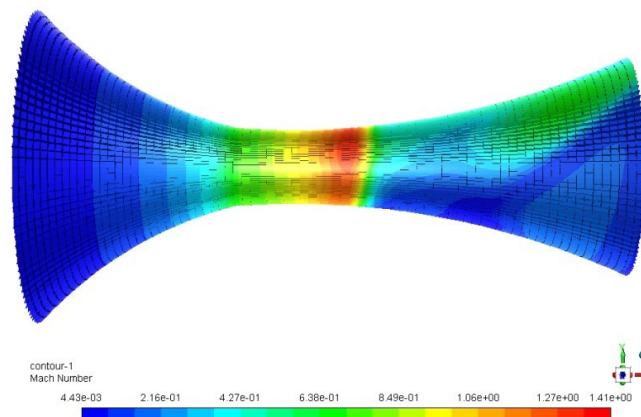
Since the shock location predicted by employing the ideal gas model is the farthest from the throat in comparison with the two real gas models, it is rational to anticipate that the maximum value of supersonic Mach number exists in the ideal gas case. The error in the magnitude of Mach number is about 21% extra for SRK model and 43% for BWR, as shown in figure 4.



(a) Ideal gas model



(b) SRK model



(c) BWR model

Figure 4. Contours of Mach number

Variation of static temperature for the three cases is illustrated in figure 5. Ideal gas model predicts the shock location farther than the real gas model. However, incorporating real gas model in the simulation predicts different location depending on the model adopted. The contour shows

that shock inception occurs earlier for BWR model compared to SRK model. However, the minimum temperature for ideal-gas model is shown to be the lowest in comparison with the real gas models ($0.453T_0$ for the ideal gas, $0.573T_0$ for SRK, and $0.71T_0$ for BWR model).

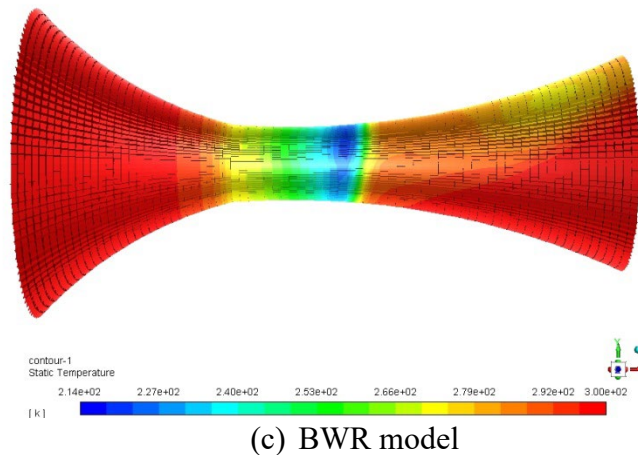
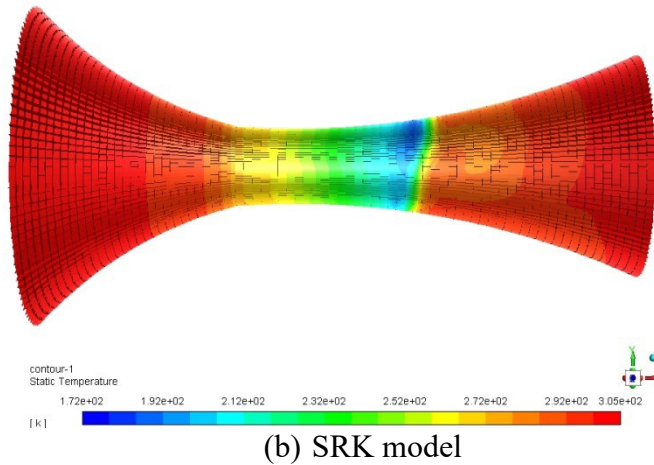
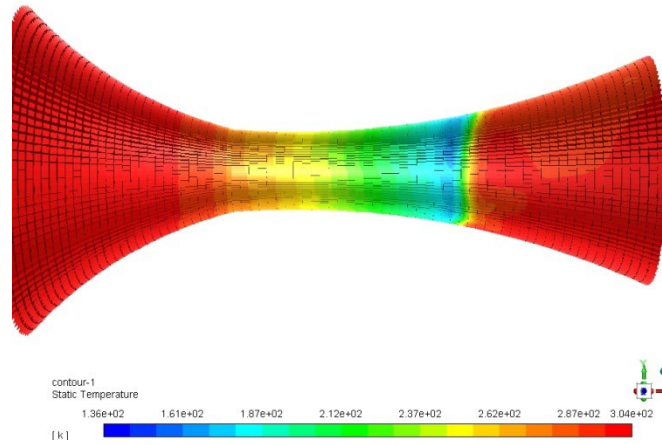
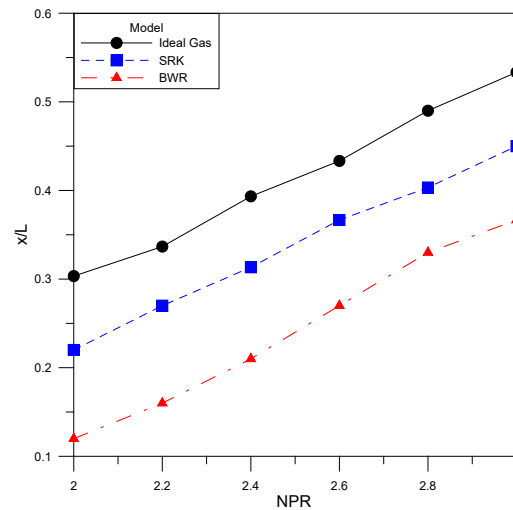


Figure 5. Contours of static temperature

Shock location

Normalized shock location is presented in Figure 6 against dimensionless NPR for the three models. The shock location is normalized w.r.t. the length of divergent part of the nozzle (L). The figure concluded that the shock position occurs near the throat when NPR is small for all models. However, Ideal gas model predicts the location farthest at prescribed NPR. BWR model, on the other hand, predicts the position of the shock closer to the throat.



Conclusion

Effect of two real gas models on the fluid properties and shock position is reported in this article by using numerical approach. The two models are compared with the ideal gas model to assess the erroneous in the prediction of shock location once assuming the gas behaves as perfect gas. The results of the simulation found that it is crucial to beware of the real gas fluid behavior when analyzing gas flow systems, particularly high-pressure flow. Comparison between perfect and real gas models showed that the ideal gas assumption would lead to serious misrepresentation of the flow field, including the position of shockwave and severe miscalculations in the design of supersonic devices.

References

- [1] Jassim, E., Abdi, M. and Muzychka, Y. (2008b) 'Computational fluid dynamics study for flow of natural gas through high pressure supersonic nozzles: part 2 - nozzle geometry and vorticity', *Journal of Petroleum Science and Technology*, Vol. 26, No. 15, pp.1773-1785. <https://doi.org/10.1080/10916460701304410>
- [2] Robert, M. N. (1903). *The Steam Turbine*. Longmans, Green, and Company, London.
- [3] Garrett, S. (2000) *From Galaxies to Turbines: Science, Technology, and the Parsons Family*. Taylor & Francis Group, England.
- [4] Jassim, E., Abdi, M. and Muzychka, Y. (2008a) 'Computational fluid dynamics study for flow of natural gas through high pressure supersonic nozzles: part 1 - real gas effects and shockwave', *Journal of Petroleum Science and Technology*, Vol. 26, No. 15, pp.1757-1772. <https://doi.org/10.1080/10916460701287847>
- [5] Jassim, E.I. (2018), 'Geometrical Impaction of supersonic nozzle on the dehumidification performance during Gas purification process -experimental study', *Arabian Journal for Science and Engineering*. <https://doi.org/10.1007/s13369-018-3340-x>

- [6] Jassim, E. and Awad, M. (2013) 'Numerical investigation of nozzle shape effect on shock wave in natural gas processing', World Academy of Science, Engineering and Technology, Vol. 78, No. 6, pp.347-352.
- [7] Kouremenos, D. A. (1986). Normal shockwaves of real gases and the generalized isentropic exponent. *Forschung im Ingenieurwesen* 52:23-31. <https://doi.org/10.1007/BF02558430>
- [8] Arina, R. (2004). Numerical simulation of near-critical fluids. *Appl. Numl. Math.* 51:409-426. <https://doi.org/10.1016/j.apnum.2004.06.002>
- [9] Bai-Shi-I, An Introduction into the Theory of Compressible Liquid Flow, Moscow: Izd. Inostrannoi Literatry, 1961.
- [10] Jassim, E.I. (2016) 'CFD study on particle separation performance by shock inception during natural gas flow in supersonic nozzle', *Progress in Computational Fluid Dynamics*, Vol. 16, No. 5, pp.300-312. <https://doi.org/10.1504/PCFD.2016.078755>